J1.6 AN INTERHEMISPHERIC COMPARSION OF CIRRUS CLOUD PROPERTIES USING MODIS AND GOES

David P. Duda*
Hampton University, Hampton, VA 23668

Patrick Minnis, William L. Smith, Jr.
Atmospheric Sciences, NASA Langley Research Center, Hampton, VA 23681

Sunny Sun-Mack, J. Kirk Ayers
Analytical Services and Materials, Inc., Hampton, VA 23666

Jean-François Gayet, Frédérique Auriol
Université Blaise Pascal, Aubière, 63177 France

Johan Ström
Stockholm University, Stockholm, S-10691 Sweden

Andreas Minikin, Andreas Petzold, Ulrich Schumann
Deutsches Zentrum für Luft- und Raumfahrt (DLR), Institut für Physik der Atmosphäre, 82230 Oberpfaffenhofen, Germany

1. INTRODUCTION

The Interhemispheric Differences in Cirrus Properties from Anthropogenic Emissions (INCA) experiment obtained aircraft-based measurements of upper tropospheric properties in the northern and southern hemispheres for comparable latitudes, seasons and backgrounds to determine any differences in cirrus clouds that may be attributable to aviation-based pollution. As a follow-up to this study, we compare ice cloud properties in the southern (without strong pollution) and northern (with strong pollution) hemisphere at mid-latitudes by using multi-spectral cloud property retrievals to compile the cirrus properties for one month each over both INCA regions (southern Chile and Scotland). Data from the Geostationary Operational Environmental Satellite (*GOES-8*) imager and the Moderate Resolution Imaging Spectroradiometer (MODIS) onboard the *Terra* satellite are used in the remote sensing retrievals. Various screening criteria are tested to minimize complicating factors such as surface differences and viewing geometry. The satellite-derived cirrus cloud properties are also compared to the aircraft-based measurements from the INCA campaign.

2. DATA

2.1 *MODIS*

The Clouds and Earth's Radiant Energy System (CERES) daytime cloud property retrieval subsystem was used to derive cloud properties from the *Terra* MODIS measurements. Radiance data from the 0.65, 1.64, 3.75, 11.0 and 12.0 μm channels at 2-km resolution were used from the MODIS instrument. The *Terra* satellite is in sun-synchronous orbit, with an equatorial crossing time at 1030 local time. For each MODIS pixel, the CERES processing system assigns a scene classification of clear or cloudy (Trepte et al., 1999), estimates of clear-sky radiance for each channel, a temperature and humidity profile, and surface elevation. Thirty-five satellite overpasses from 18 March 2001 through 15 April 2001 over southern Chile and 22 overpasses between 20 September 2000 and 17 October 2000 over northern Scotland were analyzed.

2.2 *GOES*

Four-km resolution images at 0.65, 3.9, 10.8 and 12.0 μm were collected from the GOES imager at 3-hour intervals from 19 March 2000 to 16 April 2000 over southern Chile. A total of 31 images were used in the analysis. The satellite sub-point of *GOES-8* is at 75ºW.

3. RETRIEVAL TECHNIQUE

The VIST (Visible Infrared Solar-Infrared Technique) was used to derive cloud height, optical depth, phase, effective particle size and water path for each pixel from several GOES and MODIS channels for daytime scenes (the solar zenith angle must be $\leq 78^{\circ}$). This algorithm is described in detail by Minnis et al. (1995), and an example of a VIST retrieval is presented in Figure 1.

Given the clear-sky radiance estimates for each channel and the sun/satellite geometry, the VIST computes the spectral radiances expected for both liquid-droplet and ice-water clouds for a range of particle sizes and optical depths (τ = 0.25 to 128). The effective radii r_e for the water model clouds range from 2 to 32 μm and the effective diameters D_e for the hexagonal ice

*Corresponding author address: David P. Duda, NASA Langley Research Center, MS 420, Hampton, VA 23681-2199. Email: d.p.duda@larc.nasa.gov.

column model clouds vary from 6 to 135 μm. The model cloud radiances are computed using the cloud emittance and reflectance parameterizations of Minnis et al. (1998) and a visible channel surface-atmosphere-cloud reflectance parameterization (Arduini et al., 2002). The VIST determines the cloud properties by matching the observed visible (0.65 μm), solar infrared (3.75 μm), and infrared (10.8 μm) radiances to the same quantities computed with the parameterizations and corrected to the top of the atmosphere. The process is iterative and computes results for both ice and liquid water clouds.

A combination of tests that incorporate the final cloud temperature T_c, the initially derived cloud altitude, and a reflectance ratio of 1.6 μm (if available) to 0.65 μm determine cloud phase. The phase selection is also required to be physically reasonable; no ice clouds are allowed for T_c > 273 K and no liquid clouds are permitted for T_c < 233 K.

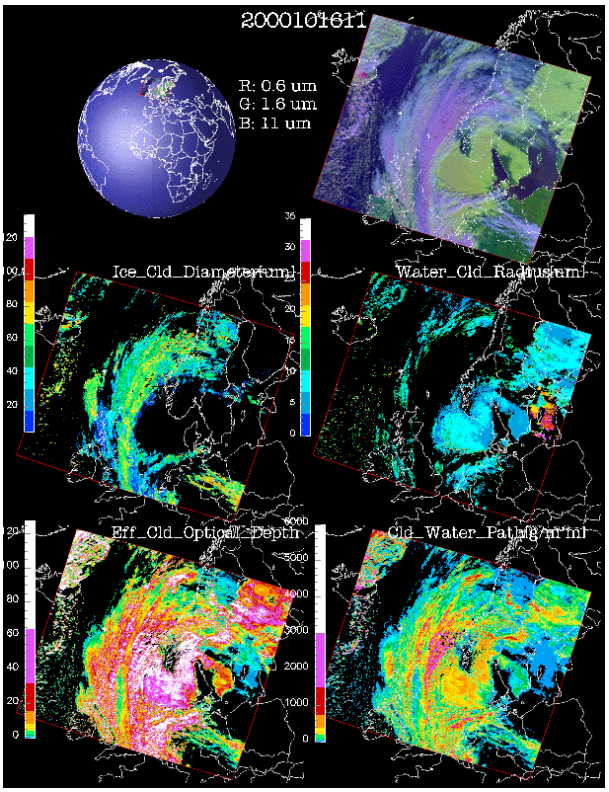

Figure 1. CERES cloud property retrieval from MODIS imagery on 16 October 2000. Top right hand figure is a 3-channel composite highlighting the water cloud (green) and ice cloud (blue) regions. The images in the second row show ice particle diameter and water droplet radius in microns, while the bottom figures present the effective cloud optical depth and cloud water path.

The cloud liquid water path *LWP* and ice water path *IWP* are derived from the retrieved values of τ and particle size. The effective cloud-top height is the altitude or pressure from the nearest vertical temperature profile that corresponds to T_c. The cloud thickness is defined using a set of crude empirical parameterizations based on τ, T_c, and altitude. Cloud base height is defined as the difference between the cloud-top height and the thickness.

The VIST retrieval algorithm has been compared to passive and active radiometric measurements at surface sites, primarily at the Atmospheric Radiation Measurement (ARM) southern Great Plains (SGP) central facility in Oklahoma (Dong et al., 1997; Mace et al. 1998; Garreaud et al. 2001). Cloud property retrievals using the VIST with the Visible Infrared Scanner (VIRS) radiances on the Tropical Rainfall Measuring Mission (TRMM) satellite show good agreement with the ground-based measurements. The mean difference between the satellite and ground-based retrievals of mean particle diameter in single-layered stratus was 1.2 μm with a standard deviation of 3.6 μm. VIST retrievals using GOES data have also compared well to *in situ* measurements of a wave cloud containing small ice crystals during the spring 1996 Subsonic Clouds and Contrails Effects Special Study experiment (SUCCESS; Young et al. 1998).

4. VALIDATION OF RETRIEVAL

To validate the satellite retrievals, we have compared the particle size results with aircraft measurements from the INCA campaign. Figure 2 presents the retrieval of ice cloud particle size during the INCA experiment on 6 October 2000 over northern Scotland. The original flight track (dashed line) of the Falcon research aircraft is superimposed on the picture. The flight path was also collocated with the satellite data by advecting the path to the time of the satellite overpass with the mean flight level wind (solid line). Only retrieved ice clouds are included in the picture.

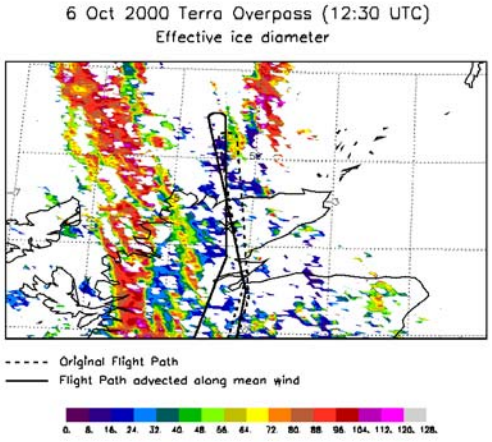

Figure 2. CERES ice cloud diameter retrieval from MODIS imagery on 6 October 2000. The cloud particle diameters are in microns. The flight track of the INCA research aircraft (Falcon, shown as dashed line) and the location of the aircraft relative to the cloud field (estimated by advecting the flight path with the mean flight level wind, solid line) during the satellite overpass are also shown.

A comparison between the satellite-retrieved ice cloud particle size and the *in situ* aircraft data is shown in Figure 3. The Falcon was equipped with several microphysics instruments including FSSP-300 (Baumgardner et al., 1992) and 2D-C (Gayet et al., 1996). The size calibration of the FSSP probe is taken from Borrmann et al. (2000). The original 31 FSSP-300 channels have been re-binned to 29 new size bins based on T-matrix calculations for ellipsoidal particles with a refractive index of 1.33. For particles in ice phase cirrus clouds, this size calibration should improve the measured size distribution compared to FSSP-300 calibrations that use spherical particles. The results from the polar nephelometer onboard the Falcon (Gayet et al., 1996) were used to determine the phase of the measured cloud particles. A particle concentration threshold of 2 particles/cm^3 was used to determine when the aircraft was in a cirrus cloud. From these measurements, time series of generalized effective diameter (D_{ge}) following the definition of Fu (1996) were computed. The computed ice cloud D_{ge} measurements (light blue plus signs) are plotted in Figure 3 with the satellite-derived ice particle diameter (solid black line). To collocate the satellite values, all retrieved satellite pixels within 4 km of the reported position of the Falcon were averaged together. For a more equal comparison with the satellite retrievals, Figure 3 also shows 20-second averages of the Falcon particle size measurements (red triangles). For the time period within a half hour of the satellite overpass of the MODIS instrument, the aircraft and satellite results indicate that the satellite-observed variations are representative of the changes occurring within the clouds.

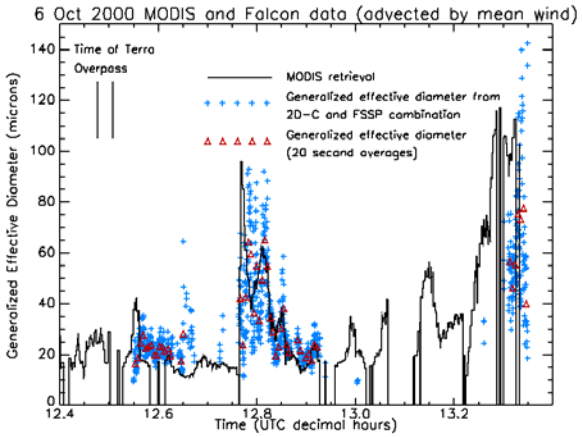

Figure 3. CERES ice cloud diameter retrieval from MODIS imagery on 6 October 2000 collocated with the generalized effective diameter (D_{ge}) measurements derived from a combination of FSSP-300 and 2-DC measurements from the Falcon. The red triangles indicate the 20-second mean values of D_{ge}.

For the segment from approximately 1246 UTC to 1256 UTC the Falcon was flying a level course through cirrus at an altitude of approximately 10.25 km. Figure 4 shows the satellite and aircraft-based ice cloud particle size retrievals for this time period, as well as the satellite-retrieved effective ice cloud top height (times a factor of 10) and the effective ice cloud optical depth (times a factor of 100). The optical depth retrievals show that the cirrus depth decreases from a peak value of 1.2 near the beginning of the segment to a value between 0.3 and 0.5 for the final two-thirds of the segment. The effective cloud height retrieval shows a generally increasing trend in height from around 7.5 km for the first third of the segment to a value near 11.0 km for the second half of the time period. The underestimation of cloud top height during the first half of the segment is consistent with the expectation that the cloud was optically thin but physically thick during this segment. Since the effective cloud height retrieval is a measure of the level of maximum IR emission in the cloud, the lower retrieved cloud top heights during the first half of the segments are a result of most of the cloud emission coming from the lower part of the cloud layer. Later in the time period as the cloud optical depth (and the physical depth) decrease, the satellite cloud top height retrieval improves as most of the IR emission comes from a more limited range of heights. Note also that as the cloud layer thins and the expected range in ice cloud particle size decreases, the comparison between the satellite and aircraft ice particle size improves.

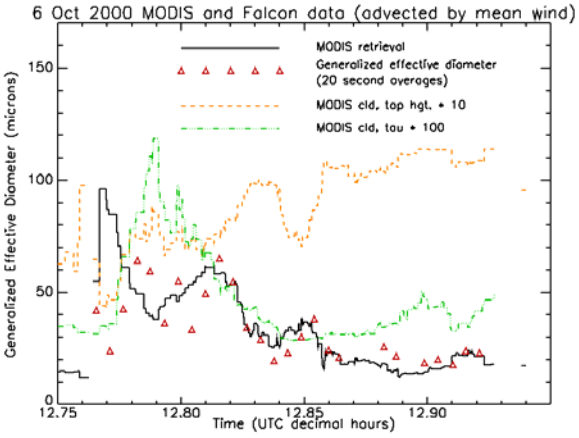

Figure 4. CERES ice cloud diameter retrieval (solid black line) from MODIS imagery on 6 October 2000 collocated with the 20-second average D_{ge} measurements (red triangles) and the CERES effective cloud top height (orange dashed line) and CERES cloud optical depth (green dotted-dashed line) retrievals.

5. RESULTS AND DISCUSSION

To compile a dataset of cirrus cloud property statistics comparable in season and location to the INCA flight observations, MODIS data from all available *Terra* overpasses within a one month period during the fall season that included the sites of the INCA field campaigns (Prestwick, Scotland and Punta Arenas, Chile) were analyzed. Several threshold criteria were used to classify clouds as cirrus and to improve the overall quality of the satellite retrievals. Only ocean pixels were included from both the GOES and MODIS retrievals to reduce satellite retrieval difficulties associated with variable surface properties. Cirrus

clouds were defined as the remaining cloudy pixels with $T_c \leq 233$ K and an $IWP \leq 20$ g m^{-2} and a cloud top height of 7 km or higher. To reduce the effect of partial cloudiness on the retrievals, no edge pixels were included in the cloud property statistics; each ice cloud pixel had to be completely surrounded by other ice cloud pixels to be considered as a valid cirrus pixel. Finally, to investigate the effects of satellite viewing zenith angle (SVZA) on the retrievals, all valid cirrus pixels were binned by SVZA (in five degree intervals) and are shown in Figure 5.

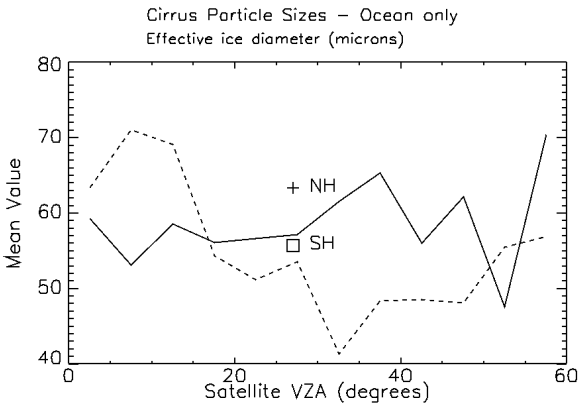

Figure 5. Mean CERES cirrus cloud particle size retrievals derived from northern hemispheric (NH, solid line) and southern hemispheric (SH, dashed line) MODIS observations as a function of satellite viewing zenith angle. The definition of cirrus is presented in the text. The plus sign and square represent the monthly means of all cirrus retrieved with a SVZA less than or equal to 60 degrees.

These MODIS results indicate a hemispheric difference in cirrus particle sizes that is opposite to the aircraft-based results from INCA, with slightly larger particles in the northern hemisphere (63.3 μm) than in the southern hemisphere (53.2 μm) analyses. The southern hemispheric analysis from the GOES observations (not shown, monthly mean of 51.9 μm) also yielded mean cirrus particle sizes smaller than those from the MODIS NH observations. Figure 5 suggests that the satellite viewing zenith angle has a strong effect on the VIST retrieval in this study. For the near-zenith viewing angles the southern hemispheric ice crystal sizes are more than 10 μm larger than the northern hemispheric results, while the opposite result occurs for larger SVZA. Some unresolved factors that may account for the larger particle sizes in the northern hemispheric cirrus are the impacts of low-cloud contamination, cloud horizontal heterogeneity and ice particle shape on the satellite retrievals.

References

Arduini, R. F., P. Minnis, and D. F. Young, 2002: Investigation of a visible reflectance parameterization for determining cloud properties in multi-layered clouds. *Proc. AMS 11th Conf. Cloud Physics*, Ogden, UT, June 3-7.

Baumgardner, D., J. E. Dye, B. W. Gandrud, and R. G. Knollenberg, 1992: Interpretation of measurements made by the forward scattering spectrometer probe (FSSP-300) during the Airborne Arctic Stratospheric Expedition. *J. Geophys. Res.,* **97,** 8035 – 8046.

Borrmann, S., B. Luo, and M. Mishchenko, 2000: Application of the T-matrix method to the measurement of aspherical (ellipsoidal) particles with forward scattering optical particle counters. *J. Aerosol Sci.,* **31,** 789 – 799.

Dong, X., T. P. Ackerman, E. E. Clothiaux, P. Pilewskie, and Y. Han, 1997: Microphysical and radiative properties of boundary layer stratiform clouds deduced from ground-based measurements. *J. Geophys. Res.,* **102** (D20), 23 829 – 23 843.

Fu, Q., 1996: An accurate parameterization of the solar radiative properties of cirrus clouds for climate models. *J. Climate,* **9,** 2058-2082.

Garreaud, R., J. Rutllant, J. Quintana, J. Carrasco, and P. Minnis, 2001: CIMAR-5: A snapsot of the lower troposphere over the subtropical southeast Pacific. *Bull. Amer. Meteor. Soc.,* **82,** 2193-2207.

Gayet, J. F., G. Febvre, G. Brogniez, H. Chepfer, W. Renger and P. Wendling, 1996: Microphysical and optical properties of cirrus and contrails: Cloud field study on 13 October 1989. *J. Atmos. Sci.,* **53,** 126-138.

Gayet, J. F., O. Crepal, J. F. Fournol, and S. Oshchepkov, 1997: A new airborne nephelometer for measurements of optical and microphysical cloud properties. Part I: Theoretical design. *Ann. Geophys.,* **15,** 451-459.

Mace, G. G., T. P. Ackerman, P. Minnis, and D. F. Young, 1998: Cirrus layer microphysical properties derived from surface-based millimeter radar and infrared interferometer data. *J. Geophys. Res.,* **103** (D18), 23 207-23 216.

Minnis, P., D. P. Kratz, J. A. Coakley, Jr. M. D. King, D. Garber, P. Heck, S. Mayor, D. F. Young, and R. Arduini, 1995: Cloud Optical Property Retrieval (Subsystem 4.3). "Clouds and the Earth's Radiant Energ System (CERES) algorithm theoretical basis document, Volume III: Cloud Analyses and Radiance Inversions (Subsystem 4)", *NASA RP 1376 Vol.* 3, pp. 135-176.

Minnis, P., D. P. Garber, D. F. Young, R. F. Arduini, and Y. Takano, 1998: Parameterization of reflectance and effective emittance for satellite remote sensing of cloud properties. *J. Atmos. Sci.,* **55,** 3313-3339.

Minnis, P., D. F. Young, B. A. Wielicki, P. W. Heck, S. Sun-Mack and T. D. Murray, 1999: Cloud properties derived from VIRS for CERES. *Proc. 10th Conf. Atmos. Rad.,* 28 June – 2 July, Madison, WI.

Trepte, Q., Y. Chen, S. Sun-Mack, P. Minnis, D. F. Young, B. A. Baum, and P. W. Heck, 1999: Scene identification for the CERES cloud analysis subsystem. *Proc. AMS 10th Conf. Atmos. Rad.,* 28 June – 2 July, Madison, WI.

Young, D. F., P. Minnis, D. Baumgardner, and H. Gerber, 1998: Comparison of in situ and satellite-derived cloud properties during SUCCESS. *Geophys. Res. Lett.*, **25,** 1125-1128.